Hindawi
Geofluids
Volume 2022, Article ID 8215223, 9 pages
https://doi.org/10.1155/2022/8215223

Research Article

Well Pattern and Well Spacing Optimization of Large Volume Water Injection in a Low-Permeability Reservoir with Pressure Sensitivity

Jie Zhan,[1,2] **Yafei Tian**,[3] **Chao Fan**,[1,2] **Xianlin Ma**,[1,2] **Ren-Shi Nie**,[3] **Dongqi Ji**,[4,5] **Teng Li**,[1,2] **and Hongyan Yu**[6]

[1]*School of Petroleum Engineering, Xi'an Shiyou University, Xi'an 710065, China*
[2]*Engineering Research Center of Development and Management for Low to Ultra-Low Permeability Oil & Gas Reservoirs in West China, Ministry of Education, Xi'an Shiyou University, Xi'an 710065, China*
[3]*State Key Laboratory of Oil & Gas Reservoir Geology and Exploitation, Southwest Petroleum University, Chengdu 610500, China*
[4]*Research Institute of Petroleum Exploration and Development, PetroChina, Beijing 100083, China*
[5]*School of Energy Resources, China University of Geosciences (Beijing), Beijing 100083, China*
[6]*State Key Laboratory of Continental Dynamics, Department of Geology, Northwest University, Xi'an 710065, China*

Correspondence should be addressed to Jie Zhan; zhanjie@xsyu.edu.cn and Xianlin Ma; xianlinm@126.com

Received 20 June 2022; Accepted 30 July 2022; Published 19 August 2022

Academic Editor: Shuyang Liu

Even with the fractured wells, the primary oil recovery of low-permeability reservoirs is still poor in Block X of Shengli Oilfield. To further enhance the oil recovery, water is injected into the reservoir. Different from the conventional injection scheme, the maximum daily injection rate of the proposed scheme by Shengli Oilfield reaches 2000 m^3, and the average daily injection rate is around 1500 m^3. Thus, the conventional well spacing of certain well pattern is not suitable for the novel injection scheme. In the paper, the optimal well pattern and well spacing for the large volume water injection scheme to develop a pressure-sensitive low-permeability reservoir is investigated. Firstly, the CMG is employed to build the basic reservoir model developed by fractured vertical wells. To finely depict the pressure sensitivity, the dilation-recompaction geomechanical model is introduced to couple with the basic reservoir model. Based on the established coupled model, the optimal well spacing for the inverted 5-spot well pattern and the inverted 9-spot well pattern is investigated with a total of 80 sets of numerical experiments. The numerical experiments indicate that the optimal well spacing for the inverted 5-spot well pattern is 850 m/350 m and the optimal well spacing for the inverted 9-spot well pattern is 550 m/450 m. To further screen the well pattern, the normalized index of oil production per unit area of each well pattern is proposed. And it is found that the oil production per unit area of the inverted 5-spot well pattern is higher than the inverted 9-spot well pattern. For the reservoir developed with fractured vertical wells coupled with large volume water injection, compared with the inverted 9-spot well pattern, the inverted 5-spot well pattern is better, and the corresponding optimal well spacing is 850 m/350 m. The paper proposes an efficient simulation and optimization workflow for the development of pressure-sensitive low-permeability reservoirs with fractured vertical wells coupled with large volume water injection, providing practical guidance for the efficient and sustainable development of pressure-sensitive low-permeability reservoirs.

1. Introduction

There are abundant low-permeability reservoirs in China and worldwide, which have become a key component in the global energy system. For instance, 46% of China's oil and gas resources are of low quality, which are mostly low-permeability reservoirs [1–4]. Due to the nature of the low-permeability reservoir, the reservoir does not perform well if the EOR/EGR technology, such as fracking and acidizing, has not been applied. Over the years, the technology of

developing low-permeability reservoirs has been significantly improved. But water injection is still the primary method to improve the performance of low-permeability reservoirs [5–8]. Shengli Oilfield proposes an innovative waterflooding scheme with large volume injection to further improve the low-permeability reservoir performance in Block X, which has been depleted for years with low productivity [9]. There are two factors accounting for the improvement of reservoir performance. On one hand, the large volume injection will increase the swept volume. On the other hand, the residual oil located in the region with high seepage resistance can be further mobilized due to the established high-pressure driven system induced by the large volume of injected water so that the displacement efficiency can be further improved. To some extent, the reservoir is rejuvenated due to the novel injection scheme. Different from the conventional injection scheme, the maximum daily injection rate of the proposed scheme by Shengli Oilfield reaches 2000 m^3, and the average daily injection rate is around 1500 m^3. Therefore, the conventional well spacing of certain well pattern is not suitable for the novel scheme, large volume water injection coupled with fractured vertical producers. The inverted 5-spot well pattern and the inverted 9-spot well pattern are widely implemented in the field. Meanwhile, the optimal well pattern and well spacing under different field conditions have been investigated based on machine learning (data-driven modeling) and numerical simulation [10–13]. But few studies have been reported on the optimization of well pattern and well spacing of the novel scheme proposed by Shengli Oilfield to develop the pressure-sensitive low-permeability. In the paper, we build up the coupled reservoir models to represent different scenarios (different well spacing for both the inverted 5-spot well pattern and inverted 9-spot well pattern of the novel scheme to develop a pressure-sensitive low-permeability reservoir) via the advanced reservoir simulator, CMG. With a total of 80 sets of numerical experiments, the optimal well spacing for both the inverted 5-spot well pattern and inverted 9-spot well pattern of the novel scheme is quantified. Then, with the proposed normalized index of oil production per unit area of each well pattern, the optimal well pattern between the inverted 5-spot well pattern and inverted 9-spot well pattern for the novel scheme is studied, as shown in the following flowchart (Figure 1). The study proposes an efficient simulation and optimization workflow for the development of pressure-sensitive low-permeability reservoirs with fractured vertical wells coupled with large volume water injection. With the methodology presented in the study, not only the field test can be further optimized, leading to more efficient and sustainable development, but also the novel scheme proposed by Shengli Oilfield can be promoted and widely applied in China and worldwide.

2. Simulation Methodology and Integrated Workflow

The governing equations of the numerical model are the mass balance equations, including accumulation term and convection term and sink/source term [14, 15]. Darcy's law, which states that fluid flow rate is directly proportional to the pressure gradient, is applied to the fluid flow in the matrix of the model. As to the fluid flow within the hydraulic fracture, the Forchheimer model with the non-Darcy coefficient is implemented to simulate a turbulent flow, accounting for the inertial effects [16–18]. Meanwhile, local grid refinement with logarithmic spacing, discretizing the reservoir to a finer degree region around hydraulic fractures and more coarsely further away from the hydraulic fractures, is coupled with the Forchheimer model to accurately depict the detailed transient fluid flow around the hydraulic fractures [19–21]. To obtain the fluid properties, the Peng-Robinson equation of state is employed. And the oil-water relative permeability of the model is generated by the analytical correlation using the endpoint data [14].

To meet the needs of finely simulating the dynamic evolution of reservoir properties for the pressure-sensitive low-permeability reservoirs, the dilation-recompaction geomechanical model is introduced to couple with the basic reservoir model. Compared with conventional flow-geomechanical coupling models [22], where complex coupling schemes, expensive computational cost, and massive input data, such as rock mechanical data and in situ stress data, get involved, the methodology employed in the study characterizes the dominating mechanism of the physical process while keeping the modeling and computational cost low. The methodology has been applied and validated by previous work to both accurately and efficiently simulate the process [9, 23–26].

The dilation-recompaction model finely depicts the relation between the porosity and reservoir pressure as a piecewise and path-dependent function, illustrated in Figure 2 [9, 27–29]. Different value is given to the compressibility according to the range of reservoir pressure. For instance, small compressibility is given to the line segment *ab*. With the gentle slope, from point *a* to point *b*, the rock experiences an elastic small change of porosity due to the change of pressure, which is reversible. As to the steep line segment *bc*, big compressibility is assigned, leading to the intense change of porosity induced by reservoir pressure, which indicates that the reservoir undergoes irreversible dilation, usually accompanied by the opening of fissures. If the pressure drops at some point during the dilation phase, two phases of compaction will occur. If the pressure remains above the recompaction pressure (P_R), reversible elastic compaction occurs in the reservoir. If the pressure continues to drop until it is below the recompaction pressure (P_R), the reservoir enters the irreversible recompaction phase, which has a larger slope than the elastic compaction. In other words, significant compaction occurs in the reservoir during the recompaction phase. The maximum porosity (ϕ_{max}) in the dilation-recompaction model is correlated with the r_{at}, which is the maximum proportional increase allowed in porosity. The residual dilation fraction (f_r) accounts for the proportion of the total dilation which is permanent and irreversible. If the lower limit of 0 is assigned to the residual dilation fraction, the increase in pore volume as a result of dilation can be fully removed. Conversely, the

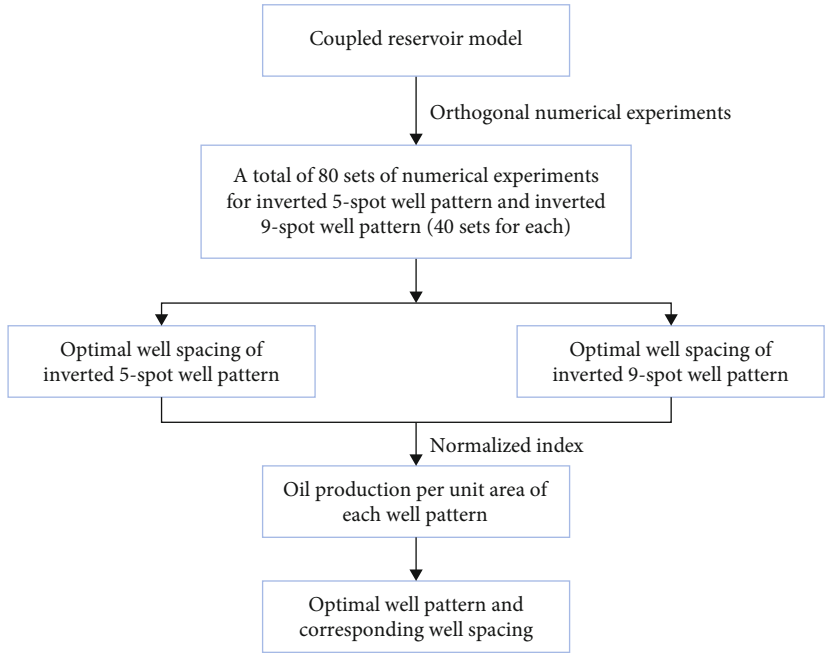

Figure 1: Flowchart of the study.

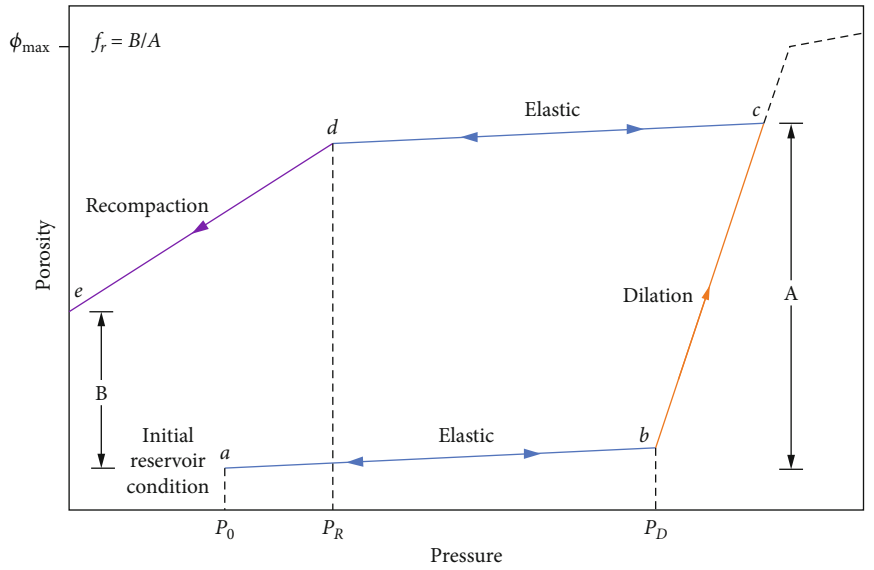

Figure 2: Dilation-recompaction model [9].

increase in pore volume induced by dilation is permanently preserved if the residual dilation fraction takes its maximum value of 1.

There is a correlation between porosity and permeability. Since the porosity evolves with the pressure, so does the permeability, which is also the feature of the low-permeability reservoir with pressure sensitivity [30, 31]. The analytical correlations for the dynamic porosity and permeability are as follows:

$$\phi = \phi_r e^{[c(P-P_R)]}, \tag{1}$$

where c is the compressibility; P_r is reference pressure; and ϕ_r is the porosity at the reference pressure.

$$K = K_0 e^{[K_{MUL}(\phi-\phi_0)/(1-\phi_0)]}, \tag{2}$$

where K_0 is the original permeability; K_{MUL} is a user-defined permeability multiplier; and ϕ_0 is the original porosity.

Based on the above simulation methodology, orthogonal numerical experiments can be conducted to obtain the optimal well spacing of each well pattern. Comparison between two types of objects (different well patterns) cannot be performed directly by the numerical simulation. To obtain the

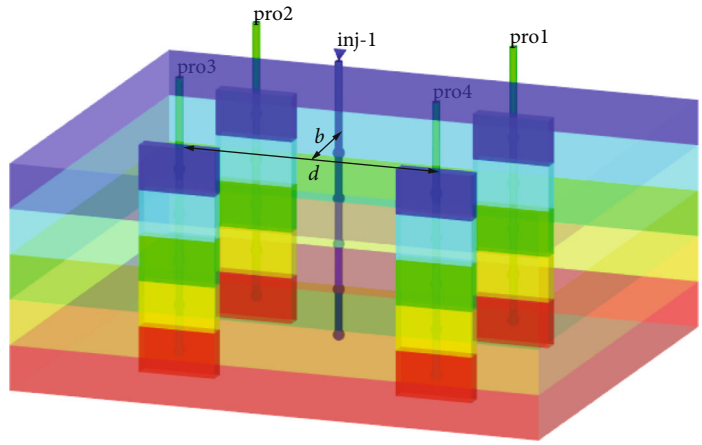

Figure 3: Three-dimensional reservoir model of inverted 5-spot well pattern.

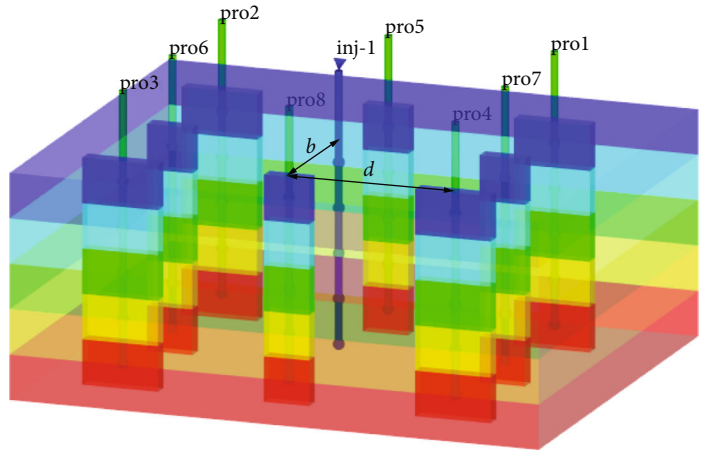

Figure 4: Three-dimensional reservoir model of inverted 9-spot well pattern.

optimal well pattern, the analytical method of reservoir engineering is introduced to couple with the numerical simulation to normalize the performance of each well pattern with optimal well spacing. That is why the normalized index is developed. The process of the analytical calculation of the normalized index is as follows. Firstly, based on the reservoir engineering method, the actual cumulative oil production of each well pattern can be determined with different weighting factors assigned to the corner well and side well, indicating the actual contribution of each well to the group [32]. Then, with the optimal spacing of each well pattern, the corresponding area of each well pattern can be acquired, which is also the area controlled by the injector. Thus, the proposed normalized index of oil production of each well pattern over the corresponding area is quantified so that the optimal well pattern can be determined. With the integrated workflow, combining the analytical method of reservoir engineering with numerical simulation, the well pattern and well spacing can be optimized simultaneously. The detailed analytical calculation will be presented in the results and discussion part.

3. Reservoir Model

Based on the CMG, the reservoir model is developed with the data of Block X. The dimensions of the numerical model are 1750 m × 1450 m × 8 m, corresponding to the length, width, and thickness of the reservoir, respectively. For the inverted 5-spot well pattern, there are one vertical injector and four vertical fractured producers, as shown in Figure 3. For the inverted 9-spot well pattern, there are one vertical injector and eight vertical fractured producers, as shown in Figure 4. d stands for the distance between wells. b stands for the distance between each row. All the wells are perforated from the top to the bottom of the reservoir. The half-length of the hydraulic fracture of the corner producer is 125 m, and the half-length of the hydraulic fracture of the side producer is 75 m. The conductivity of hydraulic fracture is 3.05 mD·m. And the cumulative water injection is 6.0×10^4 m^3. The detailed injection scheme is shown in Figure 5, which is the constraint for the injector of the numerical model. The producer is operated with a minimum bottom-hole pressure of 200 kPa, to fully harness the

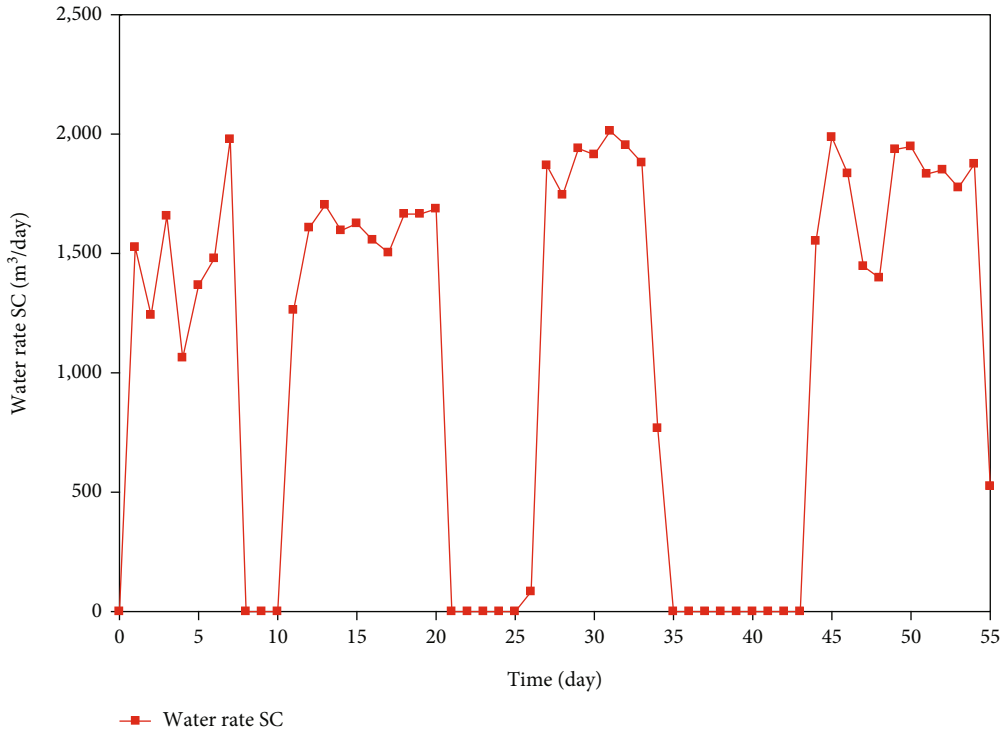

Figure 5: Daily water injection rate.

Table 1: List of model parameters.

Parameters	Value	Unit
Model dimensions	1750 × 1450 × 8	m
Thickness	8	m
Depth	3200	m
Porosity	0.13	/
Permeability	5	mD
Initial reservoir pressure	28	MPa
Reservoir temperature	123	˚C
Hydraulic fracture conductivity	3.05	mD·m
Half-length of hydraulic fracture(corner well)	125	m
Half-length of hydraulic fracture(side well)	75	m

formation energy. Due to the large volume of injected water in each slug within a few days, the bottom-hole pressure is built up rapidly, leading to the increase of the injection pressure. To stabilize the injection pressure at the wellhead within the safe operation limit, the injection is terminated for several days between each slug to facilitate the pressure diffusion outward from the injection spot. Instead of continuous injection, the water slug injection mode is employed in the field. The specific parameters used in the models are listed in Tables 1 and 2.

4. Results and Discussion

Based on the above established model, 40 simulation scenarios are developed with different well spacing for each well pattern, respectively, as shown in Tables 3 and 4. There is a total of 80 sets of numerical experiments. The simulation outcomes are illustrated in Figures 6 and 7, generated with MATLAB.

If the well spacing is too small, it will lead to higher water production with lower oil production. If the well spacing is too large, the supplemental energy by the injection cannot be utilized efficiently to improve the reservoir performance. Based on the cumulative oil production of the well group with different well spacing, the optimal well spacing for the inverted 5-spot well pattern is 850 m/350 m, and the optimal well spacing for the inverted 9-spot well pattern is 550 m/450 m, as shown in the following figures.

With the above optimal well spacing of each well pattern, the optimal well pattern will be determined between the

Table 2: Parameters used in the dilation-recompaction model.

Parameters	Value	Unit
Compressibility coefficient (C_{ab})	9.5×10^{-6}	1/kPa
Dilation compressibility coefficient (C_{bc})	8×10^{-4}	1/kPa
Residual dilation fraction (f_r)	0.1	/
Recompaction pressure (P_R)	30	MPa
Maximum allowed proportional increase in porosity (r_{at})	1.3	/
Dilation pressure (P_D)	50	MPa
Initial reservoir pressure (P_0)	28	MPa
Permeability multipliers (I/J/K) (K_{MUL})	50	/

Table 3: Orthogonal experiment design of well spacing (inverted 5-spot well pattern).

b (m)	d (m)							
	600	650	700	750	800	850	900	950
250	250 × 600	250 × 650	250 × 700	250 × 750	250 × 800	250 × 850	250 × 900	250 × 950
300	300 × 600	300 × 650	300 × 700	300 × 750	300 × 800	300 × 850	300 × 900	300 × 950
350	350 × 600	350 × 650	350 × 700	350 × 750	350 × 800	350 × 850	350 × 900	350 × 950
400	400 × 600	400 × 650	400 × 700	400 × 750	400 × 800	400 × 850	400 × 900	400 × 950
450	450 × 600	450 × 650	450 × 700	450 × 750	450 × 800	450 × 850	450 × 900	450 × 950

Table 4: Orthogonal experiment design of well spacing (inverted 9-spot well pattern).

b (m)	d (m)							
	300	350	400	450	500	550	600	650
300	300 × 300	300 × 350	300 × 400	300 × 450	300 × 500	300 × 550	300 × 600	300 × 650
350	350 × 300	350 × 350	350 × 400	350 × 450	350 × 500	350 × 550	350 × 600	350 × 650
400	400 × 300	400 × 350	400 × 400	400 × 450	400 × 500	400 × 550	400 × 600	400 × 650
450	450 × 300	450 × 350	450 × 400	450 × 450	450 × 500	450 × 550	450 × 600	450 × 650
500	500 × 300	500 × 350	500 × 400	500 × 450	500 × 500	500 × 550	500 × 600	500 × 650

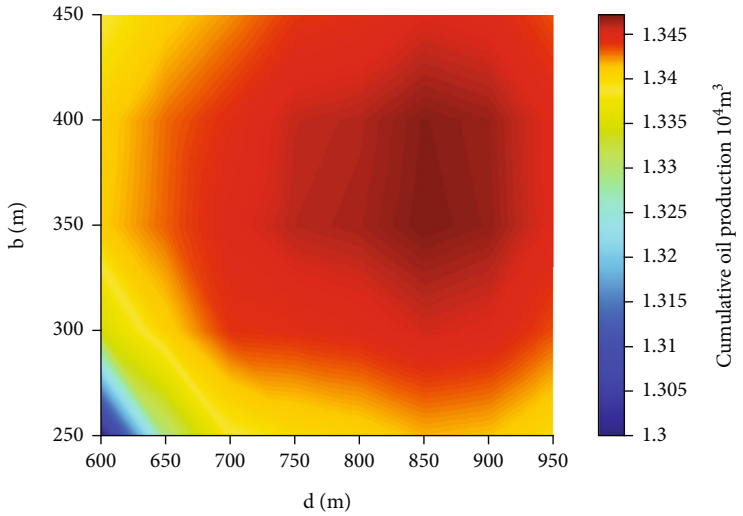

Figure 6: Cumulative oil production for the scenarios with different well spacing (inverted 5-spot well pattern).

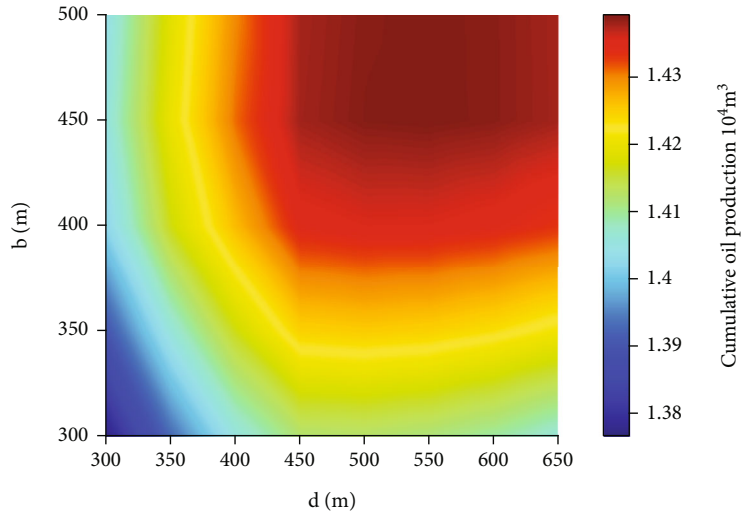

Figure 7: Cumulative oil production for the scenarios with different well spacing (inverted 9-spot well pattern).

Table 5: Evaluation of optimal well pattern.

Parameters	Notation		Inverted 5-spot well pattern	Inverted 9-spot well pattern
Area of well group (m^2)	A		595000	990000
Oil production-corner well (m^3)	N_{pc}	N_{pc1}	3405.21	1867.67
		N_{pc2}	3330.72	1723.95
		N_{pc3}	3330.72	1723.95
		N_{pc4}	3405.24	1867.67
Weighting factor-corner well	/		1/4	1/4
Oil production-side well (m^3)	N_{ps}	N_{ps1}	/	1809.67
		N_{ps2}		1721.00
		N_{ps3}		1869.24
		N_{ps4}		1809.67
Weighting factor-side well	/		/	1/2
Oil production per unit area of each well pattern (m^3/m^2)	N		5.66×10^{-3}	5.45×10^{-3}
Number of producers	n		4	8

inverted 5-spot well pattern and the inverted 9-spot well pattern with the proposed normalized index of oil production per unit area. The normalized index is determined based on the actual cumulative oil production of a well group and the area of a well group. As to the actual cumulative oil production of each well group, different weighting factors will be assigned to the different wells of the group. 1/4 will be the weighting factor of the corner well to account for the oil production contribution to the group. And 1/2 will be assigned to the side well. The analytical correlation for the normalized index is as follows. The detailed info is listed in Table 5. The oil production per unit area of the inverted 5-spot well pattern is higher than the inverted 9-spot well pattern. For the reservoir developed with fractured vertical wells coupled with large volume water injection, based on the normalized index, the inverted 5-spot well pattern is better.

Inverted 5-spot well pattern:

$$N = \frac{1/4\left(N_{pc1} + N_{pc2} + N_{pc3} + N_{pc4}\right)}{A}, \tag{3}$$

$$A = 2bd. \tag{4}$$

Inverted 9-spot well pattern:

$$N = \frac{1/4\left(N_{pc1} + N_{pc2} + N_{pc3} + N_{pc4}\right) + 1/2\left(N_{ps1} + N_{ps2} + N_{ps3} + N_{ps4}\right)}{A}, \tag{5}$$

$$A = 4bd. \tag{6}$$

5. Conclusion

In the study, based on the efficient modeling method, the numerical model of pressure-sensitive low-permeability reservoirs developed with fractured vertical wells coupled with large volume water injection is established. With the coupled model, the well pattern and well spacing optimization workflow is developed with the proposed normalized index, oil production per unit area of a certain well pattern. Based on the integrated optimization workflow, with a total of 80 sets of numerical experiments, it is found that the reservoir developed with fractured vertical wells is coupled with large volume water injection; compared with the inverted 9-spot well pattern, the inverted 5-spot well pattern is better, and the corresponding optimal well spacing is 850 m/350 m. The insights obtained from the paper will shed light on the development of low-permeability reservoirs with the novel scheme proposed by Shengli Oilfield.

Data Availability

Data is available upon request.

Conflicts of Interest

The authors declare no conflict of interest.

Acknowledgments

This research is funded by the Youth Project of the National Natural Science Foundation of China (Grant No. 52004219), the General Project of National Natural Science Foundation of China (Grant No. 51974253), the Natural Science Foundation of Shaanxi Province (Grant Nos. 2020JQ-781 and 2017JM5109), the Scientific Research Program Funded by Shaanxi Provincial Education Department (Grant No. 20JS117), the Open Fund of State Key Laboratory of Shale Oil and Gas Enrichment Mechanisms and Effective Development (Grant No. G5800-20-ZS-KFGY018), and the CNPC Innovation Fund (Grant No. 2020D-5007-0204). School of Petroleum Engineering at Xi'an Shiyou University is highly appreciated.

References

[1] J. Cai, D. A. Wood, H. Hajibeygi, and S. Iglauer, "Multiscale and multiphysics influences on fluids in unconventional reservoirs: modeling and simulation," *Advances in Geo-Energy Research*, vol. 6, no. 2, pp. 91–94, 2022.

[2] Y. Li, H. Luo, H. Li et al., "A brief review of dynamic capillarity effect and its characteristics in low permeability and tight reservoirs," *Journal of Petroleum Science and Engineering*, vol. 189, article 106959, 2020.

[3] W. Hu, Y. Wei, and J. Bao, "Development of the theory and technology for low permeability reservoirs in China," *Petroleum Exploration and Development*, vol. 45, no. 4, pp. 685–697, 2018.

[4] S. Huang, Y. Wu, X. Meng, L. Liu, and W. Ji, "Recent advances on microscopic pore characteristics of low permeability sandstone reservoirs," *Advances in Geo-Energy Research*, vol. 2, no. 2, pp. 122–134, 2018.

[5] D. Wang, D. Niu, and H. A. Li, "Predicting waterflooding performance in low-permeability reservoirs with linear dynamical systems," *SPE Journal*, vol. 22, no. 5, pp. 1596–1608, 2017.

[6] Z. Yuan, J. Wang, S. Li, J. Ren, and M. Zhou, "A new approach to estimating recovery factor for extra-low permeability waterflooding sandstone reservoirs," *Petroleum Exploration and Development*, vol. 41, no. 3, pp. 377–386, 2014.

[7] Z. Aghaeifar, S. Strand, T. Puntervold, T. Austad, and F. M. Sajjad, "Smart Water injection strategies for optimized EOR in a high temperature offshore oil reservoir," *Journal of Petroleum Science and Engineering*, vol. 165, pp. 743–751, 2018.

[8] J. Udy, B. Hansen, S. Maddux et al., "Review of field development optimization of waterflooding, EOR, and well placement focusing on history matching and optimization algorithms," *Processes*, vol. 5, no. 3, p. 34, 2017.

[9] J. Zhan, C. Fan, X. Ma, Z. Zheng, Z. Su, and Z. Niu, "High-precision numerical simulation on the cyclic high-pressure water slug injection in a low-permeability reservoir," *Geofluids*, vol. 2021, 10 pages, 2021.

[10] S. Kalam, U. Yousuf, S. A. Abu-Khamsin, U. B. Waheed, and R. A. Khan, "An ANN model to predict oil recovery from a 5-spot waterflood of a heterogeneous reservoir," *Journal of Petroleum Science and Engineering*, vol. 210, article 110012, 2022.

[11] O. Oluwasanmi, A. N. Pastor, O. Charles, N. Christopher, and O. Seyi, "Optimizing productivity in oil rims: simulation studies on water and gas injection patterns," *Arabian Journal of Geosciences*, vol. 14, no. 7, pp. 1–20, 2021.

[12] E. I. Okon, J. A. Adetuberu, and D. Appah, "Maximising oil recovery in mature water floods using automated pattern flood management," in *Proceedings of the SPE Nigeria Annual International Conference and Exhibition*, Lagos, Nigeria, 2019.

[13] J. E. Onwunalu and L. J. Durlofsky, "A new well-pattern-optimization procedure for large-scale field development," *SPE Journal*, vol. 16, no. 3, pp. 594–607, 2011.

[14] Computer Modelling Group, *User Guide*, Computer Modelling Group Ltd, 2015.

[15] Z. Chen, *Reservoir simulation: mathematical techniques in oil recovery*, Society for Industrial and Applied Mathematics, 2007.

[16] A. Arrarás, F. J. Gaspar, L. Portero, and C. Rodrigo, "Geometric multigrid methods for Darcy-Forchheimer flow in fractured porous media," *Computers & Mathematics with Applications*, vol. 78, no. 9, pp. 3139–3151, 2019.

[17] D. Takhanov, *Forchheimer model for non-Darcy flow in porous media and fractures*, Master's Thesis, Imperial College London, London, UK, 2011.

[18] R. D. Evans and F. Civan, *Characterization of Non-Darcy Multiphase Flow in Petroleum Bearing Formation. Final report*, Oklahoma Univ. School of Petroleum and Geological Engineering, Norman, OK (United States), 1994.

[19] B. Rubin, "Accurate simulation of non-Darcy flow in stimulated fractured shale reservoirs," in *SPE Western regional meeting*, Anaheim, California, USA, 2010Society of Petroleum Engineers.

[20] A. Novlesky, A. Kumar, and S. Merkle, "Shale gas modeling workflow: from microseismic to simulation–a Horn River case study," in *Canadian Unconventional Resources Conference*, Calgary, Alberta, Canada, 2011.

[21] J. Zhan, Z. Niu, M. Li et al., "Numerical simulation and modeling on co2 sequestration coupled with enhanced gas recovery in shale gas reservoirs," *Geofluids*, vol. 2021, 15 pages, 2021.

[22] A. Settari and F. M. Mounts, "A coupled reservoir and geomechanical simulation system," *SPE Journal*, vol. 3, no. 3, pp. 219–226, 1998.

[23] X. Ma, X. Chen, and J. Zhan, "Numerical simulation method for multi-stage hydraulic fracturing based on modified dilation-recompaction model," *Arabian Journal of Geosciences*, vol. 15, no. 7, pp. 1–9, 2022.

[24] R. Gao, X. Wang, Z. Yang et al., "Application of dilation-recompaction model in fracturing optimisation in tight oil reservoir," in *Proceedings of the International Petroleum Technology Conference*, Beijing, China, 2019.

[25] X. Huang, J. Wang, S. Chen, and I. D. Gates, "A simple dilation-recompaction model for hydraulic fracturing," *Journal of Unconventional Oil and Gas Resources*, vol. 16, pp. 62–75, 2016.

[26] X. Huang, *Application of dilation-recompaction model in hydraulic fracturing simulation*, Master's Thesis, University of Calgary, Calgary, Canada, 2015.

[27] C. I. Beattie, T. C. Boberg, and G. S. McNab, "Reservoir simulation of cyclic steam stimulation in the Cold Lake oil sands," in *Proceedings of the SPE California Regional Meeting*, Bakersfield, California, 1989.

[28] Y. Ito, "The introduction of the microchanneling phenomenon to cyclic steam stimulation and its application to the numerical simulator (sand deformation concept)," *Society of Petroleum Engineers Journal*, vol. 24, no. 4, pp. 417–430, 1984.

[29] B. Y. Jamaloei, "Impact of formation dilation–recompaction on cyclic steam stimulation," *SPE Reservoir Evaluation & Engineering*, vol. 24, no. 1, pp. 98–126, 2021.

[30] R. A. Farquhar, B. G. D. Smart, A. C. Todd, D. E. Tompkins, and A. J. Tweedie, "Stress sensitivity of low-permeability sandstones from the Rotliegendes sandstone," in *Proceedings of the SPE annual technical conference and exhibition*, Houston, Texas, 1993.

[31] N. H. Kilmer, N. R. Morrow, and J. K. Pitman, "Pressure sensitivity of low permeability sandstones," *Journal of Petroleum Science and Engineering*, vol. 1, no. 1, pp. 65–81, 1987.

[32] C. Li, *Fundamentals of Reservoir Engineering*, Petroleum Industry Press, Beijing, 2011.